2011 50th IEEE Conference on Decision and Control and
European Control Conference (CDC-ECC)
Orlando, FL, USA, December 12-15, 2011

Optimal LQR-based Multi-loop Linear Control Strategy for UPS Inverter Applications using Resonant Controller

A. Hasanzadeh, *Member, IEEE*, C. S. Edrington, *Senior Member, IEEE,* B. Maghsoudlou
and H. Mokhtari, *Member, IEEE*

***Abstract*-- This paper presents an optimal multi-loop control structure for uninterruptible power supply (UPS) applications which use voltage source inverter (VSI) coupled with LC filter. A resonant controller ensures tracking of sinusoidal voltage reference and rejection of sinusoidal current disturbance with no steady-state error if the loop remains stable. The challenges are reduction of output total harmonic distortion (THD), improving damping of the LC resonance frequency and preventing generation of fast closed-loop modes which go beyond the frequency range of inverter with limited switching frequency. An extension of the classic linear quadratic regulator (LQR) is proposed which addresses the optimal tracking problem. The paper also presents an improved controller to further reduce the voltage distortions for highly accurate applications. The designed controller is simulated and also experimentally built and the results are presented to confirm analytical derivations.**

***Index Terms— UPS inverter, optimal tracking, LQR, LC filter, resonance frequency, multi-loop design*.**

I. Introduction

Uninterruptiblepower supply (UPS) systems are used to provide continuous high quality power to critical loads such as medical equipment. In a UPS, the inverter output is connected to the load through a low-pass LC filter which filters the high frequency switching pulses and provides a smooth signal at the linear or nonlinear loads terminal. The output voltage control objective is to track a sinusoidal input reference voltage with low THD and regulated voltage RMS for all range of load variations.

The LC filter has a resonance frequency which corresponds to a pair of poorly damped poles in the system transfer function. Such phenomenon can lead to undesired oscillations or even instability if not properly addressed. The damping can be improved either passively by adding appropriate resistors or actively by using suitable controls [1-2]. It is challenging to provide enough damping to those poles with an output feedback alone [3]. Thus, multi-loop strategies have been widely used which use inverter current or capacitor current as feedback signal in addition to the load voltage. Some methods also use load current feed-forward as well as time-derivatives of the reference signal to achieve better performance [4].

A. Hasanzadeh and C. S. Edrington (corresponding author) are with The Center of Advanced Power Systems, Florida State University. Email: hasanzadeh@caps.fsu.edu, edrington@caps.fsu.edu. B. Maghsoudlou and H. Mokhtari are with the Sharif University of Technology. Email: benyamin_maghoudlou@yahoo.com, mokhtari@sharif.edu.

The conventional multi-loop techniques use proportional (P) and proportional-integrating (PI) type of controller for single-phase systems which are not suitable [5]. The resonant controller has the advantage of nullifying the steady-state error and also rejecting the sinusoidal disturbances [6]. In the UPS model, the load current can be envisaged as such a disturbance where the resonant controller can ensure desired steady-state operation for linear loads. When the load draws distorted current, however, multiple resonant units can be employed within the controller structure for high level of THD reduction.

This paper proposes a new method for designing the resonant controllers within a multi-loop control system. The proposed method is based on extending of the classical LQR of optimal control theory to address the tracking problem involved in the UPS inverter system. The formulation presented in this paper provides an easy, yet powerful, method of tuning the controller gains no matter how numerous they are. This advantage is used to design a multi-resonant controller to reduce the output voltage THD level.

Several control methods for UPS inverters have been reported in the literature. Those include robust, deadbeat, repetitive, sliding mode, neural networks, adaptive, optimal control etc [5,7-9]. A multi-loop scheme with resonant controller is used in [10] where the controller gains are adjusted using the characteristic ratio assignment (CRA). It is concluded in [10] that THD levels are not satisfied for a nonlinear load. Method of [8] uses the LQR technique to adjust a multi-loop scheme. That scheme is however dependent on the LC filter parameters and also needs measurement of the load current. The LQR technique is also used in [9] to adjust a multi-loop scheme which is based on PI controller and time-derivative of the reference signal in a set of parallel inverters. Reference [11] uses the LQR technique in combination with the deadbeat control to improve damping of an LCL filter used to connect a three-phase source to the grid. A similar approach is presented in [12].

In this paper, UPS inverter power and control stages are outlined in Section II. A novel, advanced and unified method is introduced in Section III. Improvement of the controller to reduce the THD level for highly accurate applications is discussed in Section IV. Simulation and experimental results are presented in Section V and VI.

II. UPS Inverter System

This section provides the basic materials related to the UPS inverter power and control systems.

978-1-61284-799-3/11/$26.00 ©2011 IEEE

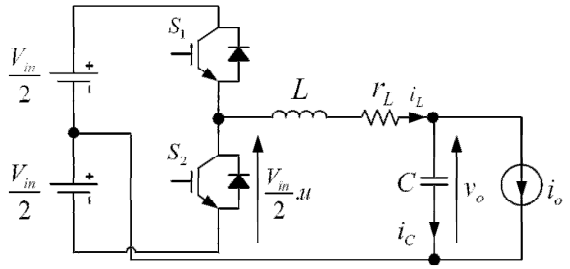

Fig. 1. Power circuit of the single-phase UPS inverter.

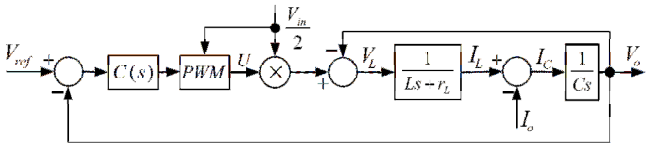

Fig. 2. Single-loop UPS inverter control system.

A. UPS Inverter Mathematical Model

Figure 1 shows the power stage of a single-phase inverter which includes an IGBT half-bridge configuration and an LC is thus filter. The differential equations that describe the dynamic behavior of this converter are

$$L\frac{di_L}{dt} = \frac{V_{in}}{2}u - v_o - r_L i_L \qquad i_C = C\frac{dv_o}{dt} = i_L - i_o \tag{1}$$

where u is the control variable which can take values of 1, 0 or -1 depending on the state of switches S_1 and S_2.

Taking average from (1) over one switching frequency, one can find the plant state-space equations as:

$$\dot{x_p} = A_p x_p + B_p u + B_w w \qquad y_p = C_p x_p + D_p u \tag{2}$$

Where

$$A_p = \begin{bmatrix} \frac{-r_L}{L} & \frac{-1}{L} \\ \frac{1}{C} & 0 \end{bmatrix} B_p = \begin{bmatrix} \frac{V_{in}}{2L} \\ 0 \end{bmatrix} \qquad x_p = \begin{bmatrix} i_L \\ v_o \end{bmatrix} \quad y_p = v_o$$
$$C_p = [0 \quad 1] \quad D_p = 0 \qquad B_w = \begin{bmatrix} 0 \\ \frac{-1}{C} \end{bmatrix} \quad w = i_o \tag{3}$$

B. UPS Inverter Control System

A single-loop control strategy is shown in Fig. 2. The control objectives in this system are to achieve (i) output voltage regulation which means low RMS steady-state error, (ii) fast transient response, and (iii) low total harmonic distortion (THD), for all variations of the load and system parameters' changes and uncertainties such as the DC voltage, the inductor and capacitor of the LC filter, resistances.

Note that the command waveform and also the disturbance signal are both sinusoids at the fundamental frequency. A so-called proportional-resonant (PR) controller given by

$$G(s) = K_0 + \frac{K_3 s + K_4}{s^2 + {\omega_o}^2} = P_{(Controller)} + R_{(Controller)} \tag{4}$$

is thus suitable for the system shown in Fig. 2 where ω_o is the system frequency.

The LC filter has a poorly damped resonant frequency at $\omega_r = 1/\sqrt{LC}$ having a damping ratio equal to $\zeta = \frac{r_L}{2}\sqrt{C/L}$. This generates undesired high-frequency oscillations at the output voltage if not properly controlled. A PR controller of the form (4) cannot provide enough damping of the LC-filter

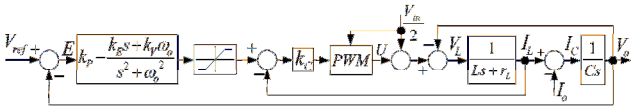

Fig. 3. Conventional multi-loop UPS control structure using inverter current

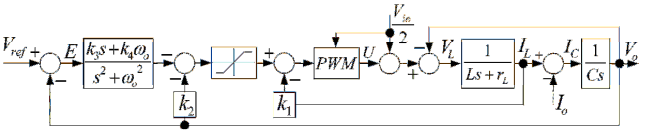

Fig. 4. Modified multi-loop UPS control structure using inverter current

resonant frequency. Thus, the controller must be equipped with further terms such as appropriate lead compensators $C(s) = G_{PR}(s)G_{Load}(s)$. Proper design of the lead compensator is also challenging. Alternative method is to use a multi-loop structure such as what is shown in Fig. 3.

A salient advantage of using a multi-loop control structure is the possibility of using state-feedback techniques such as the LQR method. In Fig. 4, notice that the P controller is moved from the PR into the inner loop for convenience of design. The PR controller adds two zeros to the system while the R controller adds only one zero. This also has the advantage of introducing -20 dB/dec in the magnitude curve for high frequencies which lowers the bandwidth and makes the loop more robust to high frequency noises. A state-space representation for this transfer function of R compensator is given by $\dot{x_c} = A_c x_c + B_c e$ where $e = v_{ref} - y_p$ and

$$A_c = \begin{bmatrix} 0 & -\omega_o \\ \omega_o & 0 \end{bmatrix} B_p = \begin{bmatrix} 1 \\ 0 \end{bmatrix} \tag{5}$$

The control signal can now conveniently be written as

$$u = -[k_1 \quad k_2 \quad k_3 \quad k_4] \begin{bmatrix} x_p \\ x_c \end{bmatrix} = -Kx \tag{6}$$

By augmenting the inverter and the R controller variables, and assuming $v_{ref} = 0$, the following state-space representation is obtained for the closed-loop system.

$$\dot{x} = Ax + Bu \qquad u = -Kx \tag{7}$$

where

$$A = \begin{bmatrix} 0 & \frac{1}{C} & 0 & 0 \\ \frac{-1}{L} & \frac{-r_L}{L} & 0 & 0 \\ -1 & 0 & 0 & -{\omega_o}^2 \\ 0 & 0 & 1 & 0 \end{bmatrix} \quad B = \begin{bmatrix} 0 \\ \frac{V_{in}}{2L} \\ 0 \\ 0 \end{bmatrix} \tag{8}$$
$$u = -[k_{11} \quad k_{12} \quad k_{13} \quad k_{14}]x$$

This is a regulation problem and the LQR method can be used to obtain the vector K Matrix Q is a diagonal 4×4. The closed-loop system is surely stable (for every positive semi-definite matrix Q) but its transient response depends on matrix Q. We are particularly interested in a solution which results in desired tracking response. Such a constraint is not formulated within the LQR structure.

III. Direct Solution to Optimal Tracking Problem

The LQR which can only solve a "regulation" problem while in this section shows that the LQR concept can be extended to directly address the optimal tracking problem [13-14]. Using this method, the admissible q_i's are obtained with less effort and with a more transparent view on the problem. Moreover, the method is applicable to higher-order controllers without excessive complexity.

A. Mathematical Formulation

The tracking problem can generally be put in the following framework. Assume that y^* is the command signal and y is the output signal. The direct tracking can be defined as follows: Derive the controller u such that the following index is minimized

$$J(u) = \int_0^\infty (he^2 + v^2)\, dt \tag{9}$$

where $e = y^* - y$ is the tracking error, $v = \Delta(u)$ is a transformed input and $h > 0$ is the weight of tracking term in the cost function. The new (or transformed or pseudo) input v must be properly defined to ensure that the cost function is well-defined that means the cost function is convergent.

In the case of the UPS inverter system, the command signal y^* is a pure sinusoidal signal at frequency ω_o. This means that all signals will be sinusoids at frequency ω_o at steady-state. Thus, they (including y^*, y and u) all satisfy the equation $\ddot{a} + \omega_o^2 a = 0$. Thus, let's define

$$\Delta u = v = \ddot{u} + \omega_o^2 u = 0 \tag{10}$$

In the steady-state, $v = 0$, but during the transient-time, this equation is not held. Thus, v in (10) is an index of how far the signal is from the desired value at time instant t.

Now to formulate a solution to this problem, it is possible to redefine the state variables in this system in order to transform the tracking problem into a regulation problem as follows. The

augmented vector of state variables is $x = [x_p^T \quad x_c^T]^T$. Define $z = \ddot{x} + \omega_o^2 x$. Considering the definition of x_c, z can be written in the form of $z = [\ddot{x}_p + \omega_o^2 x_p \quad \dot{e} \quad \omega_o e]^T$. Then it is straightforward to show that z satisfies the following state-space representation

$$\dot{z} = Az + Bv \qquad\qquad v = -Kz \tag{11}$$

where K=$[k_1 \quad k_2 \quad k_3 \quad k_4]$. Definitions for matrices A and B remain unchanged. Also notice that the index function can be rewritten as

$$J(u) = \int_0^\infty (he^2 + v^2)\, dt = \int_0^\infty (z^T Q_1 z + v^2)\, dt \tag{12}$$

where

$$Q_1 = diag\{q_1, q_2, q_3, q_4\} = diag\{0,0,0, h/\omega_o^2\} \tag{13}$$

This means that the tracking problem has been transformed to a regulation problem with the Q_1 matrix in (13) and can now directly be addressed by the LQR technique.

B. Selecting Q Matrix

Significance of the proposed method is that it reduces design of the controller gains to the design of LQR gains matrix Q. For example, in the tracking index, the parameter h which is equal to $\omega_o^2 q_4$ directly controls the tracking error. Increasing this parameter reduces the tracking error. Then, q_3 controls rate of change of tracking error and can thus smoothen undesired fast oscillations on the response. The coefficients q_2 and q_1 provide further control on voltage and current signals. Having said this, a design can be reached by subsequently increasing q_i's and observing their impacts on the response. The characteristics which are of importance in the UPS inverter application are as follows.

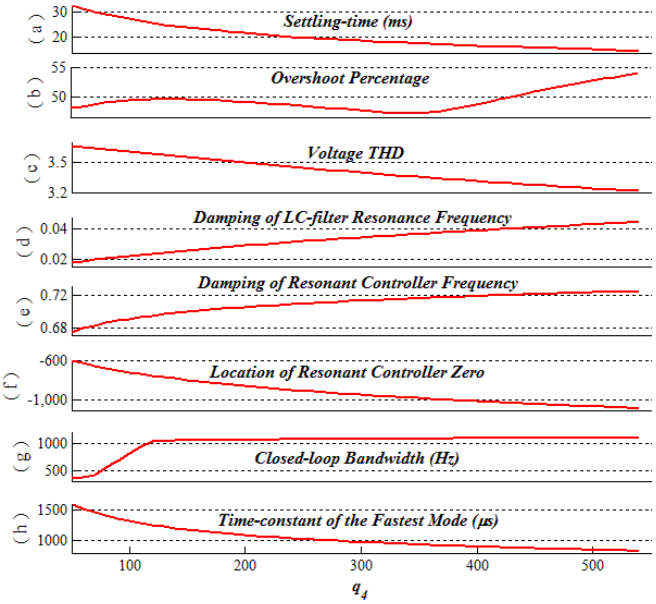

Fig. 5. Monitoring the closed-loop characteristics when q_4 varies and $q_1 = q_2 = q_3$=0: (a) settling time in ms (b) overshoot in percentage (c) THD in percentage (d) damping of LC resonance mode (e) damping of R controller mode (f) system's zero (g) time-constant of the system's fastest mode in μs.

TABLE I
PARAMETERS OF THE UPS INVERTER POWER STAGE

$L = 0.8\, mH,\ r_L = 0.1\, \Omega,\ C = 40\, \mu F,\ V_{in} = 760\, V,\ f_s = 20\, kHz,$
$f_o = 50\, Hz,\ V_o = 220\, V_{rms},\ Load\ (1\emptyset\ \ 1KVA\ \ \ PF = 0.8)$

1) Speed is represented by the settling-time of the response to a change in load or in reference signal.

2) Overshoot shows the excessive increase in the response in percentage of its amplitude.

3) Voltage THD is caused by nonlinearities in the system mainly those caused by the nonlinear loads.

4) Damping of LC resonance mode shows how far the controller can avoid undesired oscillations caused by the LC resonance mode.

5) Damping of R controller mode shows whether the R controller modes have adequate damping.

6) System's zero which is generated by the R controller and is preferred to remain minimum-phase with adequate distance from origin.

7) Closed-loop bandwidth must be large enough to ensure strength of control signal and low enough to avoid excessive sensor noise propagation.

8) PWM switching frequency poses limitation on the PWM generated signal. A highly fast changing control signal cannot be generated by a low switching frequency. This means that the loop must not have fast modes beyond the capacity supported by the switching frequency.

Using UPS inverter power stage parameters of table I, the design begins with increasing q_4 and which has the most significant impact on the tracking error. Figure 5 shows the above eight characteristics of the system versus q_4. Figure 5(a) shows that the settling-time of the response decreases from 30 ms to about 15 ms when q_4 is increased to 500. The overshoot remains within a range of 45 to 55%, part (b). The output THD gradually decreases from 3.7% to 3.2% as shown in (c). The THD is calculated for a highly nonlinear load which draws a current with THD of about 50%. The damping of the LC-filter resonance mode is gradually

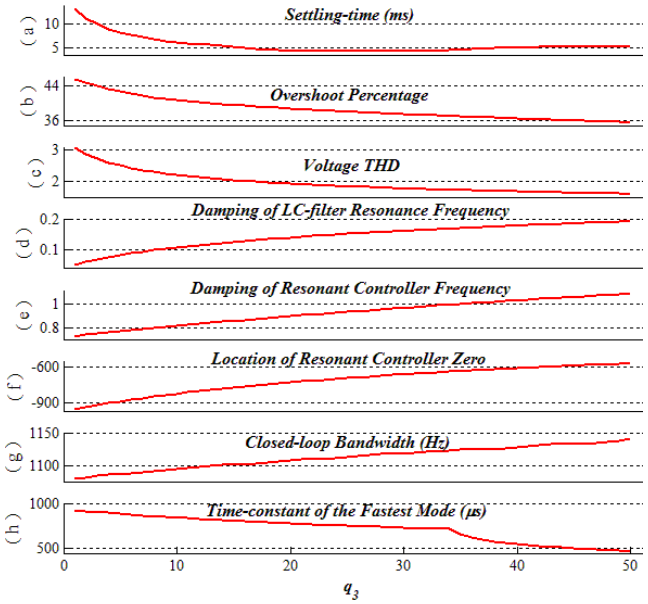

Fig. 6. Monitoring the closed-loop characteristics when q_3 varies and $q_1 = q_2 = 0$, $q_4 = 350$: (a) settling time in ms (b) overshoot in percentage (c) THD in percentage (d) damping of LC resonance mode (e) damping of R controller mode (f) system's zero (g) time-constant of the system's fastest mode in μs.

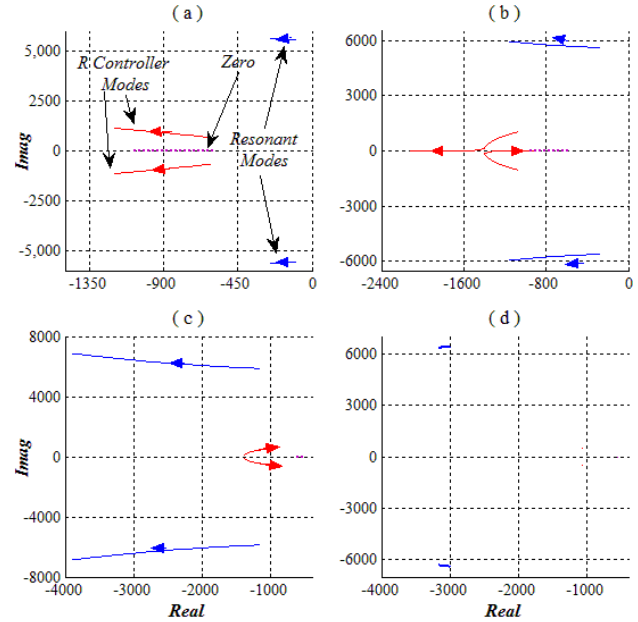

Fig. 7. Loci of the closed-loop poles and zero versus (a) $50 \le q_4 \le 500$, $q_1 = q_2 = q_3 = 0$ (b) $5 \le q_3 \le 50$, $q_1 = q_2 = 0$, $q_4 = 350$ (c) $0 \le 10^6 q_2 \le 20$, $q_1 = 0$, $q_3 = 30$, $q_4 = 350$ (d) $0 \le 10^6 q_1 \le 20$, $q_2 = 10^{-5}$, $q_3 = 30$, $q_4 = 350$

increasing from 0.02 to 0.045. Damping of the R controller mode is also gradually increasing as shown in (e). The system's zero is shown in part (f) which exhibits movement towards left hand side of the complex plane. The closed-loop bandwidth grows to about 1000 Hz which is just above the open-loop resonance frequency as shown in (g). Part (h) shows the time-constant of the fastest mode in the closed-loop system. This mode is important to be observed carefully because the PWM cannot generate fast changing control signals due to limitation in the switching frequency. A switching frequency of 20 KHz corresponds to a switching time of 50 μs. A rule-of-thumb consideration is that several switching cycles must be placed within the time-constant of the fastest mode in order to be generated successfully. This means that the fastest time-constant must not go below, say, 300 μs.

At this stage, q_4 can be selected for example at 350 and the same procedure is repeated for q_3. Results are shown in Fig. 6. It is observed that increasing q_3 has the following desired results: reduction in settling-time, reduction in overshoot, and reduction in output THD, increase in the damping of LC-filter mode. The trade-off is in increase of system's zero, increase in bandwidth, and reduction in the time—constant of the system's fastest mode. A value of $q_3 = 30$ is desired.

The loci of closed-loop system poles and zero provides much insight into the design process. Such a locus when q_4 varies from 50 to 500 is shown in Fig. 7(a) and when q_3 varies from 5 to 50 is shown in part (b). These graphs confirm results exhibited in Fig. 5 and 6.

At this stage of design where q_4 and q_3 have been selected, the closed-loop characteristics are as follows: settling time about 5 ms, overshoot about 35%, THD just below 2% for a highly nonlinear current, damping of the LC-resonance mode about 0.15, and time-constant of the fastest mode about 750 μs. Next step is to adjust q_2. The system characteristics versus q_2 and q_1 can be performed similar to q_4 and q_3 to figure out related results like Fig. 5-6. The desired impacts of increasing q_2 are as follows: reduction in overshoot, reduction in THD, tremendous increase in damping of the LC resonance mode. The trade-offs are gradual decrease in speed, movement of zero towards origin, decrease in bandwidth and decrease in the time-constant of the fastest mode. A value of $q_2 = 10^{-5}$ seems desirable and is chosen here. No considerable improvement is achieved by increasing q_1 and thus, it is set at zero. The loci of poles and zero of the closed-loop system is shown in Fig. 7(c) and the closed-loop poles and zero loci is shown in Fig. 7(d). The controller gains eventually settle to about $K = [0.0167 \quad 0.0027 \quad -9.4 \quad -17.1]$.

IV. Improved Controller for Reducing THD

An attractive feature of the control strategy shown in Fig. 4 is the possibility of upgrading it to highly reduce the output voltage THD if desired. The harmonics at the output voltage are mainly due to the nonlinear loads which draw a distorted current. Since the current is considered as a disturbance signal, the controller may be improved as

$$C(s) = \sum_{n \epsilon H} \frac{K_{3n} s + K_{4n}(n\omega_o)}{s^2 + n^2 {\omega_o}^2} \qquad (14)$$

where H is the set of harmonics which are present. Such a controller completely removes all the harmonics in the set H. The controller structure becomes complicated as H becomes larger. Typically, $H = \{1,3,5,7,9\}$ is adequate for most applications and this significantly reduces the voltage THD to comply with the Standards.

A main challenge with a high order controller such as that of (14) is appropriate tuning of its gains [15]. The proposed technique of Section IV can easily be extended to address such a challenge. To show that, write the controller state-

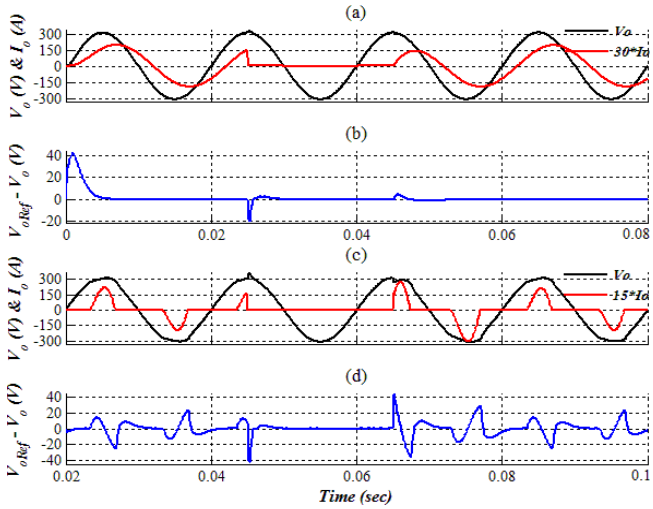

Fig. 8. A load is switched from full-load to no-load and again to full-load at times $25ms$ - $45ms$ and $45ms$ - $65ms$ for linear (a-b) and nonlinear (c-d) loads, respectively. (a, c) load voltage and current (b, d) tracking error.

TABLE II
REDUCTION OF OUTPUT VOLTAGE THD

	THD
[0.0167 0.0027 -9.4 -17.066 0 0 0 0 0 0 0 0]	3.6
[0.02 0.004 -15.9 -11.25 -2.85 -19.28 0 0 0 0 0 0]	2.8
[0.0236 0.0054 -17.35 -8.88 -13.1 -14.45 1.27 -19.45 0 0 0 0]	2.3
[0.027 0.007 -17.95 -7.6 -16.15 -10.9 -10.4 -16.5 3.6 -19.15 0 0]	1.8
[0.03 0.009 -18.28 -6.8 -17.6 -8.5 -14.5 -13 -6.4 -18.4 -3.1 -19.3]	1.32

space representation as $\dot{x_c} = A_c x_c + B_c e$ where
$A_c = blockdiag\{A_{c_1}, A_{c_2}, \dots, A_{c_N}\}$, $B_c = [B_{c_1}^T, \dots, B_{c_N}^T]^T$
In which $A_{c_N} = \begin{bmatrix} 0 & -n\omega_o \\ n\omega_o & 0 \end{bmatrix}$, $B_{c_N} = \begin{bmatrix} 1 \\ 0 \end{bmatrix}$.

The plant and controller, when augmented, will have the following state-space representation

$$\dot{x} = Ax + Bu + B_1 v_{ref} \tag{15}$$

where

$$A = \begin{bmatrix} A_p & 0 \\ -B_c C_p & A_c \end{bmatrix} \qquad B = \begin{bmatrix} B \\ 0 \end{bmatrix} \qquad B_1 = \begin{bmatrix} 0 \\ B_c \end{bmatrix} \tag{16}$$

Similar to what was developed in Section IV, define $x = [x_p^T \quad x_c^T]^T$ and $z = \ddot{x} + {\omega_o}^2 x$. Then obviously, $z = [(\ddot{x}_p + \omega_o^2 x_p)^T \quad \dot{e} \quad \omega_o e \quad z_1]^T$ where z_1 shows the states related to harmonic controllers. Also define $v = \ddot{u} + \omega_o^2 u$. With this new set of state variables and input, the whole system's state-apace representation is $\dot{z} = Az + Bv$ where A and B are defined above. Moreover, $v = -Kz$ which shows a regulation problem. The matrix Q is now having the form

$Q = diag\{q_1, q_2, \dots, q_{2k-1}, q_{2k}\}$ $\quad N_{Harmonic\ Order} = 2k$

The controller gains are conveniently obtained by similar approach according to Subsection III for q_4, q_3, q_2 and q_1. Furthermore, the other pair elements of Q matrix such as $q_5 - q_6$, $q_7 - q_8$, ... and $q_{2k-1} - q_{2k}$ are achieved similar to predetermined elements of $q_3 - q_4$ to reject undesired output voltage harmonics by appropriate adjust of corresponding resonant controller coefficients.

V. SIMULATION RESULTS

To verify performances of the proposed controllers in a realistic scenario, the UPS inverter system by Table I power stage parameters and tuned controllers' gains with the proposed control algorithms are simulated using EMTDC/PSCAD simulation software. The UPS inverter supplies both linear and nonlinear loads in compliant with IEC 62040-3 standard for class-I UPS. Figure 8 shows the case where the load switching occurs from full-load to no-load and again to full-load at times $25ms$ - $45\ ms$ and $45ms$ - $65\ ms$ for linear and nonlinear loads, respectively. The load voltage, the load current and the tracking error signals are shown. The controller exhibits desired responses.

Another simulation verifies effectiveness of the multiple resonant controllers in reducing the voltage THD. Five cases are considered: one resonant controller at fundamental frequency, two resonant controllers at fundamental and third harmonic, three resonant controllers at fundamental, third and fifth harmonics, four resonant controllers at fundamental, third, fifth and seventh harmonics, and five resonant controllers at fundamental, third, fifth, seventh and ninth harmonics. The output voltage THD for these five cases is summarized in Table II with the controller gains of vector K.

VI. EXPERIMENTAL RESULTS

Based on Table I power stage parameters, a 1kVA-UPS inverter is built and tested to experimentally verify the performance of the proposed control method. The control logic is realized and implemented using TMS320F2808, 32-bit fixed-point 100-MHz Digital Signal Processor (DSP) from Texas Instruments (TI). The control signal is applied by Pulse-Width-Modulated (PWM) approach using the DSP PWM block. The proposed controller is developed by C^{++} in Code Composer Studio (CCS) V3.3 environment (supplied by TI). Then, the program is compiled and transmitted by XDS510LC emulator into DSP Flash with USB protocol. A photograph of the experimental setup is shown in Fig. 9 which has two UPS inverters and only used one of them in this study.

First, experimental test is performed by supplying a linear load with a power factor of 0.8. Figure 10 shows the start-up transient of the UPS inverter output voltage and current connected to the linear load. Response shows a fast and smooth behavior with a THD as low as 0.5%. Next, Fig. 11 shows the UPS inverter output voltage and current when connected to the non-linear load compliant with IEC 62040-3 standard for class I UPS. The effectiveness of multiple resonant controllers in reducing the THD is experimentally verified through Fig. 13 where the resonant controllers at the third, fifth, seventh and ninth harmonics are placed within controller. The total THD is reduced to about 1%. This closely matches what was already obtained by computer simulations.

VII. CONCLUSION

The paper presented a multi-loop control structure and introduced an efficient method of optimally designing its gains for UPS inverter applications. Unlike conventional methods, we extended the LQR technique from regulation to the tracking problem. The controller removes the steady-

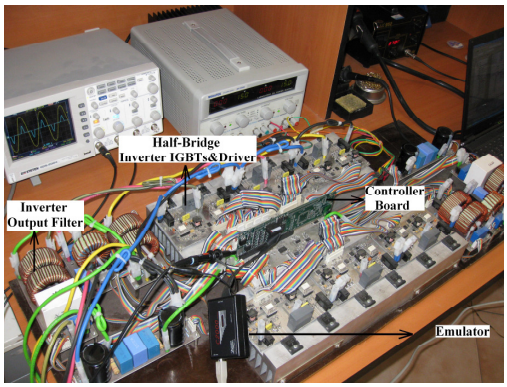

Fig. 9. Picture of the UPS inverter experimental setup

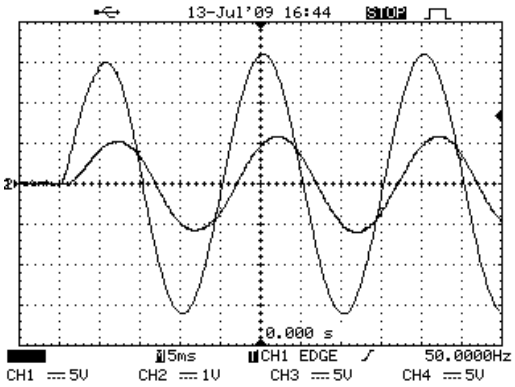

Fig. 10. Start-up transient of the UPS to linear load (Ch-1: Output Voltage waveforms, Y axis: 100V/div, Ch-2: Output Current waveform, Y axis: 5A/div, X axis: 5ms/div)

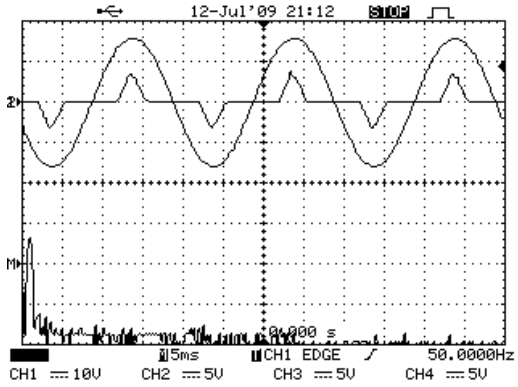

Fig. 11. Elimination of the third, fifth, seventh and the ninth harmonics (Ch-1: Voltage waveforms, Y axis: 200V/div, Ch-2: Current waveform, Y axis: 25A/div, X axis: 5ms/div MATH: Load voltage frequency spectrum, X axis: 250Hz/div, Y axis: 20dB/div)

state error, provides fast and smooth response to load changes, is robust to uncertainties in system parameters and improves damping of the resonance frequency. The controller is further improved for reduction of output voltage distortions. It is simple to apply and avoids complicated classical Bode diagrams and/or root-locus design techniques without any stability concerns while offering an optimal solution with adequate gain and phase margins. Consistent results obtained from simulations and experimental tests confirm validity of the analytical results.

ACKNOWLEDGMENT

The authors would like to thank Dr. M. Karimi Ghartemani of Sharif University of Technology, Tehran, Iran, for his valuable discussion. Additionally, we would like to thank the Florida State University's Institute for Energy Sustainability and Economic Studies for funding the effort.

REFERENCES

[1] V. Blasko and V. Kaura, "A Novel Control to Actively Damp Resonance in Input LC Filter of a Three-Phase Voltage Source Converter", *IEEE Transactions on Industry Applications*, Vol. 33, No. 2, March/April 1997, pp.542-550.

[2] P. A. Dahono, Y, R. Bahar, Y. Sato, and T. Kataoka, "Damping of transient oscillations on the output LC filter of PWM inverters by using a virtual resistor", *4th IEEE International Conference on Power Electronics and Drive Systems*, 2001, Vol. 1, pp. 403- 407.

[3] Yun Wei Li, "Control and Resonance Damping of Voltage-Source and Current-Source Converters with LC Filters", *IEEE Transactions on Industrial Electronics*, vol. 56, no. 5, May 2009, pp. 1511-1521.

[4] M. J. Ryan, W. E. Brumsickle and R. D. Lorez, "Control Topology Options for Single-Phase UPS Inverters", I*EEE Transactions on Industry Applications*, Vol. 33, No. 2, March/April 1997, pp. 493-501.

[5] H. Deng, R. Oruganti and D. Srinivasan, "Modeling and Control of Single-Phase UPS Inverters: A Survey", *IEEE PEDS*, 2005, pp. 848-853.

[6] B. A. Francis and W. M. Wonham, "The internal model principle of control theory", *Automatica*, Vol. 12, pp. 457-465, 1976.

[7] P. Mattavelli, "An Improved Deadbeat Control for UPS Using Disturbance Observers", *IEEE Transacions on Industrial Electronics*, Vol. 52, No. 1, Feb. 2005, pp. 206-212.

[8] H. Kmurcugil, O. Kukrer and A. Doganalp, "Optimal Control for Single-Phase UPS Inverters Based on Linear Quadratic Regulator Approach", SPEEDAM 2006, pp. S8-24-29.

[9] X. Sun, L-K. Wong, Y-S. Lee and D. Xu, "Design and Analysis of an Optimal Controller for Parallel Multi-Inverter Systems", *IEEE Transactions on Circuits and Systems II*, Vol. 52, No. 1, Jan 2006, pp. 56-61.

[10] Y. T. Woo and Y. C. Kim, "A Digital Control of a Single-Phase UPS Inverter for Robust AC-Voltage Tracking", *The 30th Annual Conference of the IEEE Industrial Electronics Society*, Nov. 2004, pp. 1623-1628.

[11] E. Wu and P. W. Lehn, "Digital Current Control of a Voltage Source Converter with Active Damping of LCL Resonance", *IEEE Transactions on Industrial ELectronics*, Vol. 21, No. 5, Sep. 2006, pp. 1364-1373.

[12] F. Huerta, E. Bueno, S. Cobreces, F.J. Rodriguez, and C. Giron, "Control of grid-connected voltage source converters with LCL filter using a Linear Quadratic servocontroller with state estimator", *Power Electronics Specialists Conference*, PESC 2008, pp. 3794 - 3800.

[13] B. D. O. Anderson and J. B. Moore, *Linear Optimal Control,* Englewood Cliffs, NJ: Prentice-Hall, 1971.

[14] M. G. Safonov and M. Athans, "Gain and Phase Margin for Multiloop LQG Regulators", *IEEE Transactions on Automatic Control*, vol. 22, no. 2, April 1977, pp. 173-179.

[15] M. Castilla, J. Miret, J. Matas, L. Garcia de Vicuna, and M. Guerrero, "Control Design Guidelines for Single-Phase Grid-Connected Photovoltaic Inverters With Damped Resonant Harmonic Compensators", *IEEE Transactions on Industrial Electronics*, vol. 56, no. 11, April 2009, pp. 4492-4501.